Energy transitions and time scales to equipartition in the Fermi-Pasta-Ulam oscillator chain

J. DeLuca and A. J. Lichtenberg
Department of Electrical Engineering and Computer Sciences and the Electronics Research Laboratory, University of California, Berkeley, California 94720

S. Ruffo
Dipartimento di Energetica, Università di Firenze, 50100 Firenze, Italy and Istituto Nazionale di Fisica Nucleare, Sezione di Firenze, Italy

(Received 14 October 1994)

We study the energy transitions and time scales, in the Fermi-Pasta-Ulam oscillator chain, at which the energy E, initially in a single or small group of low-frequency modes, is distributed among modes. The energy transitions, with increasing energy, are classified. At low energy the linear parts of the energies are distributed in a geometrically decreasing series $E_h = \rho^2 E_{h-2\gamma}$, with γ the mode in which most of the initial energy is placed and $\rho = (3\beta E_\gamma)/(4\pi\gamma)$. A transition occurs at $R \equiv 6\beta E_\gamma (N+1)/\pi^2 \sim 1$, with N the number of oscillators and β the quartic coupling constant. Above this transition there is strong local coupling among neighboring modes with a characteristic resonant frequency $\Omega_b \sim 4\beta\gamma E_\gamma / N^2$. There is a second transition at a critial energy $\beta E_c \sim 0.3$, above which stochasticity among low-frequency resonances transfers energy into high-frequency resonances by the Arnold diffusion mechanism. Above this transition we numerically determine a universal scaling for the time scale to approach equipartition among the modes. The universal time scale is qualitatively explained in terms of the driving time scale $\tau_b = 2\pi/\Omega_b$ and a diffusive filling time.

PACS number(s): 05.45.+b

I. INTRODUCTION

Coupled oscillator chains form good test systems for investigating energy exchange among degrees of freedom, diffusion, ergodicity on energy surfaces, and equipartition. In particular, the Fermi-Pasta-Ulam (FPU) system, consisting of a set of equal masses coupled to nearest neighbors by nonlinear springs, has been extensively studied. Fermi, Pasta, and Ulam [1], in 1954, reported the first numerical study on a chain of coupled oscillators, with a quartic nonlinearity. They observed, for a particular initial energy distribution, that the oscillators did not relax to the equipartition state, but displayed a persistent recurrence to the initial condition, contrary to the equipartition hypothesis of statistical mechanics. The results were later explained in terms of beating among the system modes (superperiod) and the superperiod was theoretically calculted using perturbation theory [2–5]. A theoretical prediction of a threshold to equipartition was obtained by Izraelev and Chirikov [6] using an "overlap" criterion for the modes. They predicted a critical energy E_c', of the initial excitation, for widespread stochasticity. For energy in a few low-frequency modes they found $E_c' \propto N$, where N is the number of oscillators (number of modes) in the chain.

Subsequently there have been many studies of the interchange of energy among modes and of energy thresholds to give approximate equipartition among modes [7–11]. Pettini and Landolfi [10] have studied the dependence of the time to equipartition on the energy of the excitation at relatively high energies, finding a relaxation time $\tau \propto N$ and a threshold for equipartition $E_c' \propto N$. The observed scaling agreed with the mode overlap hypothesis. However, equipartition that takes place on a slower time scale, at lower energy, would not have been readily observed. Kantz, Livi, and Ruffo [11] (henceforth KLR) studied the transitions and time scales to equipartition. For energy in initial modes around mode number γ, with $\gamma \propto N$, they found a transition to equipartition at a critical energy E_c, independent of N. For this initial condition they found that a time scale $\tau \propto N$ (at constant E) was requied to attain some constant measure of equipartition. As we shall see in Sec. II, this is consistent with theoretical predictions and results using other initial conditions.

In another study DeLuca, Lichtenberg, and Lieberman [12] (henceforth DLL) developed theoretical descriptions, valid in various energy ranges, which were compared to numerical results. Both the transition, with energy, to observe equipartition and the time scale required to attain a constant measure of equipartition were studied. The results of theory and numerics were in qualitative agreement and also in general agreement with results by KLR. We reserve the presentation of the details of these results to Sec. II. The main idea is that resonant interaction of a few low-frequency modes in which most of the energy resides can lead to local superperiod beat oscillations that are stochastic. The transition to stochastic local interaction occurs at

$$R \equiv (N+1)\frac{6\beta}{\pi^2}E \simeq 1 , \tag{1}$$

where β is the nonlinearity parameter of the FPU Hamiltonian [see Eq. (3)]. Since $R \propto N+1$, the energy at which

this transition occurs becomes vanishingly small as $N \to \infty$. With increasing local energy, the oscillation frequency increases until a strong Arnold diffusion mechanism can transfer energy to the higher-frequency modes, leading to equipartition. The transition was predicted to occur at a value of $E = E_c$, independent of N, which was confirmed numerically. The beat frequency has the form

$$\Omega_b \sim \gamma \beta E / N^2 \tag{2}$$

whose inverse gives a centrally important time scale for the analysis.

The modified Korteweg–de Vries (mKdV) equation approximately describes low-frequency modes of the FPU system if $\beta > 0$ and N is sufficiently large. Driscoll and O'Niel [13] showed that an instabilty of a low-frequency mode (soliton) of the mKdV equation corresponds to exponential growth in the FPU system. However, we would not expect this instability to be directly related to equipartition involving the high-frequency modes, as the differential equation does not describe these modes. DLL compared the onset of instabilty in the rescaled parameters of the mKdV equation, as found by Driscoll and O'Neil, to the parameters governing the interaction among the low-frequency FPU modes. The rescaling gives the relationship $R \simeq (8/\pi^2)(\gamma/2)^2 q^2 K^2(q^2)$, where q is the argument of the cnoidal function that describes the soliton, $\gamma - 1$ is the number of nodes of the cnoidal function, and $K(q^2)$ is the complete elliptic integral. The instability appears for $q^2 \gtrsim 0.25$ ($K = 1.7$) for $\gamma = 2$, obtaining $R \gtrsim 0.6$, which is approximately the same value as that which produced a separatrix layer in the local resonance interaction. (See Sec. II B.) We note also that a relation is found to exist between the existence of an instability in the sine-Gordon equation and mode spreading in an oscillator chain which corresponds to the discretized sine-Gordon equation [14].

In recent work [15] the mKdV differential equation was studied in the large-amplitude limit in which the nonlinear term dominates over the dispersion. In this case a shock develops rather than a soliton. The time scale to form the shock from an initial traveling wave was determined and found to be the inverse of Ω_b given in (2). The shock is, of course, mode mixing, reinforcing the importance of the inverse beat frequency to the stochastic transfer of energy among modes in the finite-N system.

The overlap of two adjacent low-frequency modes, which also leads to stochastic diffusion, occurs at a much higher value of energy, i.e., with $E/N \sim 1$. Although this criterion does not necessarily predict transfer of energy to high-frequency modes on computationally observable time scales, the energy satisfying mode overlap is generally much higher than E_c and furthermore increases continually with increasing N. The time scale for the interaction is $\tau \sim 2\pi/\omega_\gamma \simeq 2N/\pi\gamma$, which gives much faster diffusion to higher modes. As already mentioned, observations on this fast time scale, e.g., [7–9], have found a transition to equipartition from a single low-frequency mode scaling as $E_c' \propto N$. This emphasizes the importance of observing equipartition on the correct time scale for the relevant phenomenon. Along with the measure of equipartition, Pettini and Landolfi [10] also looked at the largest Lyapunov exponent $\lambda_{\max}$ of the system, finding a change of scaling with E at $E/N \sim 1$. In the work that follows we are concerned primarily with energies for which $E/N < 1$.

In the following section we will organize, by increasing energy, the various interaction phenomena that occur in the FPU oscillator chain and the time scales associated with these phenomena. The proposed mechanisms will be explained in terms of previous theoretical results and the numerical evidence. Outstanding questions, resulting from either a lack of correspondence between theory and numerics or from conflicting numerical results, will be brought out. Then, in Sec. III, numerical reuslts will be presented to answer some of the open questions. In the numerical work we concentrate our attention on initial conditions in which the energy is placed in one or a few of the lowest-frequency modes.

II. BASIC PHENOMENA, ENERGY TRANSITIONS, AND TIME SCALES

We study the quartic FPU Hamiltonian, representing a linear chain of equal masses coupled by nonlinear springs with a quartic nonlinearity [1,16],

$$H = \sum_{i=1}^{N} \tfrac{1}{2} p_i^2 + \tfrac{1}{2}(q_{i+1} - q_i)^2 + \tfrac{1}{4}\beta(q_{i+1} - q_i)^4 . \tag{3}$$

We consider the case of strong springs ($\beta > 0$) and fixed boundaries $q_0 = q_{N+1} = 0$. In the linear case ($\beta = 0$) the chain of oscillators may be put in the form of N independent normal modes and is therefore integrable and nonergodic. Those normal modes are [3,5]

$$q_i = \left[\frac{2}{1+N}\right]^{1/2} \sum_{\alpha=1}^{N} \sin\left[\frac{\pi i \alpha}{N+1}\right] Q_\alpha, \quad i = 1, \ldots, N \tag{4a}$$

$$\Omega_\alpha = 2 \sin\left[\frac{\pi\alpha}{2(N+1)}\right] , \tag{4b}$$

where Ω_α is the frequency of the αth linear mode, Q_α is its amplitude, and $\alpha = 1, \ldots, N$. We will refer to those coordinates as the "linear modes" of the system, even though they are not separable modes if we include the quartic term. The FPU Hamiltonian in the linear mode coordinates is calculated to be

$$H = \sum_{i=1}^{N} \tfrac{1}{2}(P_i^2 + \Omega_i^2 Q_i^2) + \frac{\beta}{(8N+8)} \sum_{r,s,m,n} G(r,s,m,n) Q_r Q_s Q_m Q_n , \tag{5}$$

where r, s, m, n are integers running from 1 to N and G is defined by

$$G(r,s,n,m) \equiv \Omega_r \Omega_s \Omega_n \Omega_m \sum_P B(r+s+n+m) , \tag{6}$$

with B given by

$$B(\alpha) = \begin{cases} 1 & \text{if } \alpha = 0 \\ -1 & \text{if } \alpha = \pm 2(N+1) \\ 0 & \text{otherwise} \end{cases} \tag{7}$$

and $\sum_P$ in (4) represents the sum over all eight permutations of the sign of s, n, and m. We see then that there is a selection rule for mode coupling via the quartic term.

To numerically study the FPU system, initial conditions have been used for which all the energy is concentrated in a few modes around some mode γ or in which a packet of modes has been used of width $\Delta\gamma$ in which both γ and $\Delta\gamma$ are proportional to N. In numerical experiments the time average of the linear energies E_i, $i=1,\ldots,N$, is usually calculated (see Sec. III for details). The information entropy [17,18]

$$S=-\sum_{i=1}^{N} e_i \ln e_i \ , \tag{8}$$

where $e_i=E_i/\sum_1^N E_i$ are the normalized average energies, is then introduced. Two normalized measures of equipartition have been employed. The most often used measure is [7–11]

$$\eta=\frac{S_{\max}-S(t)}{S_{\max}-S(0)} \ , \tag{9}$$

where $S_{\max}=\ln N$ (equipartition). We see from (9) that $\eta=1$ when $S(t)=S(0)$ and $\eta\to 0$ as $S(t)\to S_{\max}$, although fluctuations limit η to some finite value [18]. For N large and the initial energy in a few modes, η does not distinguish between equipartition and a plateau in which only some fraction of the N modes are occupied, but is well behaved if some fraction of N initial modes are excited. An alternative measure used by DLL is to define the effective number of modes by [17]

$$n_{\text{eff}}\equiv \exp S \ . \tag{10}$$

The normalized parameter n_{eff}/N is related to η, for a single mode initial condition, by

$$\eta=\frac{\ln N-\ln n_{\text{eff}}}{\ln N}=\frac{-\ln(n_{\text{eff}}/N)}{\ln N} \ . \tag{11}$$

We see that $\eta\to 0$ as $n_{\text{eff}}/N\to 1$, but η also becomes small as N becomes large, even if n_{eff}/N is significantly less than one.

We consider the scaling of the energy transitions between various physical phenomena observing, as appropriate, individual linear mode energies and using the macroscopic parameter n_{eff}/N. We concentrate our attention on initial conditions in which the energy is initially in one or a few low-frequency linear modes. In Sec. III we give more detailed numerics for this initial condition.

A. Low energies

At low energies, for which no significant long-time energy diffusion among modes is numerically observed, perturbation theory describes the overall pattern of the mode energy distribution. DLL found that the average linear energies decay in a geometric progression

$$E_h\simeq\rho_h^2 E_{h-2\gamma} \ , \tag{12}$$

where an average value of ρ_h over modes ρ is given approximately by

$$\rho=\left[\frac{\pi R}{8\gamma(N+1)}\right]=\frac{3\beta E}{4\pi\gamma} \ . \tag{13}$$

DLL checked the scaling for two values of γ, at constant E and for a single value of $N=32$, obtaining a geometric energy fall-off among the most strongly coupled modes, in qualitative agreement with (12) and (13). However, the scaling with E and any possible scaling with N was not checked. There is also a secondary effect of local spreading among adjacent modes that is not well understood. In an earlier work [7], in which the energy was placed in a few adjacent low-frequency modes, the geometric fall-off was also observed, but with additional local broadening as expected from the additional couplings. In Sec. III we numerically investigate the scaling in (12) and (13) both with the initial energy in a single mode and in additional neighboring modes.

A related question is the time scale to establish the geometric pattern. Since the time scale is related to the establishing of the nonlinear mode, it would be expected to be related to the inverse mode frequency $\omega_\gamma^{-1}=2N/\pi\gamma$. This is indeed the case for the low-frequency modes. However, perturbation theory shows that a longer time $t\sim 2N^2/\pi\gamma(\gamma+1)$ is required to establish the geometric progression among the highest-frequency modes. We will present some evidence for this two-time-scale behavior in numerical results given in Sec. III.

B. Low-energy transition

A single nonlinearity parameter $R=6\beta(N+1)E_\gamma/\pi^2$ governs the local interactions among low-frequency modes, where R measures the nonlinear correction ($\omega_{\text{NL}}=\gamma R/N^3$) of the linear beat ($\omega_{\text{L}}=\gamma\pi^3/N^3$) of modes ($\gamma-1$, γ, and $\gamma+1$). Examining the reduced Hamiltonian of four consecutive modes around mode γ, DLL found for the two strongest resonances of this Hamiltonian that for $R\simeq 1$, an elliptic and hyperbolic pair of fixed points appear in one resonance, giving rise to a local libration frequency $\Omega_b\simeq 6.2\gamma R/N^3\simeq 3.7\beta\gamma E_\gamma/N^2$ around the elliptic fixed point. The interaction between Ω_b and the second low-frequency resonance produces a stochastic separatrix layer connecting the hyperbolic points, which becomes large at $R\simeq 4$. For large N numerical studies indicate that most initial conditions lie in these stochastic layers [19]. The exact values of frequency and R vary with initial conditions, but only weakly. The criterion that R be sufficiently large to give widespread stochasticity within a resonance could be referred to as an "overlap criterion." The system is, however, intrinsically degenerate, such that the stochasticity arises from a more complicated set of interactions (see [16], Sec. 2.4). The overlap of these four modes does not lead to equipartition on computationally observable time scales. Numerically it is found that increasing R leads to an increase in the effective number of low-frequency modes that are stochastically interacting, giving approximately $n_{\text{eff}}\simeq 0.5R+1$. This is readily understood in terms of local mode interaction in which an increasing

number of neighboring mode resonances can form as their associated energies exceed $R \sim 1$.

C. Intermediate-energy transition

In addition to the stochastic diffusion among the low-frequency modes we expect the stochasticity to drive Arnold diffusion along stochastic layers to other modes, with the particular channels and rates to be determined by the coupling coefficients. Since the driving frequency for diffusion is associated with Ω_b, a fundamental time scale for numerical observations is

$$\tau = 2\pi/\Omega_b \propto N^2/\gamma\beta E_\gamma \ . \tag{14}$$

Using resonant normal form perturbation theory to investigate the couplings to the high-frequency modes, DLL found that, above a critical value $E > E_c$, the ratio of the stochastic drive frequency Ω_b to a high mode number beat frequency $\Delta\Omega_{12} = \gamma\pi^2/N^2$ becomes of order unity. The Arnold diffusion rate depends exponentially on the frequency ratio as $\exp(-\pi\Delta\Omega_{12}/2\Omega_b)$. Hence, for $\Omega_b \sim \Delta\Omega_{12}$, we would expect to obtain a strong diffusion of energy to high-frequency modes and equipartition on computationally observable time scales. Numerically both KLR and DLL find this transition, with a value of $E_c \approx 3$, for $\beta = 0.1$, giving $\Omega_b \approx 0.2\Delta\Omega_{12}$. This is consistent with a transition to numerically observable diffusion.

The time scales to obtain some fractional equipartition were investigated by plotting $\eta(t)$ versus a normalized time scale in KLR and by plotting $n_{\text{eff}}(t)$ versus a normalized time scale in DLL. The normalized time scale in KLR, for the initial energy in modes with $\gamma \propto N$, was Et/N. This is equivalent to normalizing to τ_b, since $Et/N \propto \gamma Et/N^2$. How well the normalization made the data at different values of E and N coincide was somewhat obscured by the fact that η only weakly discriminates among time scales near equipartition. For $E \sim E_c$ the normalized time scale in DLL was $\gamma t/N^2$. Since for $E \sim E_c$ the E scaling is not studied, this scaling is also coincident with normalizing the time to τ_b. The results by DLL were in reasonable agreement with the expected $t \propto \tau_b$ scaling, but were only checked over a small range of N between 32 and 128.

For $E \gg E_c$ (but $E/N < 1$) KLR found, for an initial condition with the energy in a few low-frequency modes, that by setting $\tau = t/N$ the scaling became nearly universal when $\eta(t)$ was plotted vs E/N. We note that this result $\eta(t/N, E/N) = \text{const}$ can also be interpreted, through rescaling, as the existence of a universal time scale $\eta(t/\tau_b) = \text{const}$, where $\tau_b \simeq N^2/\gamma\beta E_\gamma$. This is consistent with the scaling by DLL at a fixed energy $E \simeq E_c$. The result can be somewhat obscured at large N, near equipartition, because of the relation given in (11). We investigate this scaling in detail in Sec. III.

D. High-energy transition

For an energy such that

$$\frac{\gamma\beta E_\gamma}{N} \gtrsim 1 \ , \tag{15}$$

the low-frequency modes interact strongly to create stochasticity on a time scale

$$\tau \sim N/E_\gamma \ . \tag{16}$$

Since the mode containing most of the energy has a frequency shift comparable to the frequency spacing between modes, this interaction has been referred to as an overlap criterion. However, as previously mentioned, the actual interaction is more complicated for this intrinsically degenerate system. For large N, the energies satisfying (15) are much higher than those involved in the resonance interactions. Investigating equipartition on the fast time scale of (16), Pettini and Landolfi [10] found that equipartition occurs when (15) is satisfied. They also examined the largest Lyapunov exponent λ_m, finding a transition with increasing energy from $\lambda_{\max} \propto E^2$ to $\lambda_{\max} \propto E^{2/3}$, the latter associated with a random matrix approximation. This indicates diffusion across resonances, through the entire phase space. In the next section, we limit our numerical investigation to energies below the transition given in (15), so that the scaling results are not contaminated by the fully stochastic regime.

III. NUMERICAL EVIDENCE

We present the following numerical evidence in support of the picture developed in the preceding section. Although considerable numerical results are available from earlier work, some of it summarized in the previous sections, specific calculations help to clarify the individual physical concepts. As in Sec. II, we systematically scan through the energy ranges, with particular emphasis on energy transitions and time-scales. We concentrate our attention on initial conditions in which energy is placed in one or a few of the lowest-frequency modes. In all numerical studies β is held to a fixed value $\beta = 0.1$. The theory indicates that β is simply a scaling factor such that all energy transitions scale inversely with β.

Two numerical procedures are used to obtain the data. In the first, following KLR, the leapfrog algorithm is used to integrate the equations of motion. The mode energies are determined in a time window sufficiently wide to average over mode oscillation times, but not over longer-time resonance frequencies. To smooth the data a set of initial conditions (typically ten), with the same energy but different oscillator phases are separately integrated and averaged. In the second numerical procedure, following DLL, a fourth-order symplectic integrator is used to integrate a single initial condition, with the smoothing obtained by long-time averaging of the energies. For a steady-state mode distribution the two procedures give very similar results, with the long-time averaging being smoother, i.e., mode fluctuations or oscillations on all time scales but the integration time itself are averaged over. For an evolving mode distribution the results are somewhat different, as the long-time integration is an integral of the results obtained in a time window. Thus, for evolving mode distributions we have used the first procedure to unambiguously present results at a given time, but recognize that oscillations longer than the averaging time may make the interpretation

more difficult. The second procedure is generally used for steady-state observations, except when a specific comparison calls for the use of the first procedure. For Figs. 1–4, in which an equilibrium is reached, the integrated procedure is used to obtain results independent of local fluctuations. For Figs. 5–8, in which time-dependent phenomena are presented, the first procedure is employed.

A. Low energy

In Fig. 1 we investigate the scaling of ρ with E and N. Equations (12) and (13) indicate that the geometric ratio is proportional to E and independent of N. We use the same initial condition as DLL in which 90% of the energy is in mode $\gamma=3$ and 10% is divided between modes 2 and 4. In Fig. 1(a), for $E=0.1$ and $N=32$, 64, and 128 ($R=0.2$, 0.4, and 0.8), numerical results are compared with the predicted value of ρ (solid line), obtaining reasonable agreement. In Fig. 1(b), for $E=1.5$ and $N=32$, 64, and 128 ($R=3$, 6, and 12), the numerical results no longer agree with theory. Perturbation theory no longer holds, as there is a strong low-frequency interaction, when $R \gtrsim 1$. We have also numerically investigated the time scale to form the geometric ratio, finding that the low-frequency modes attain the energy in a time $T_{\mathrm{LF}} \sim 2N/\pi\gamma$, while the highest-frequency modes require a longer time $T_{\mathrm{HF}} \sim 2N^2/\pi\gamma(\gamma+1)$, results which are in good agreement with perturbation theory.

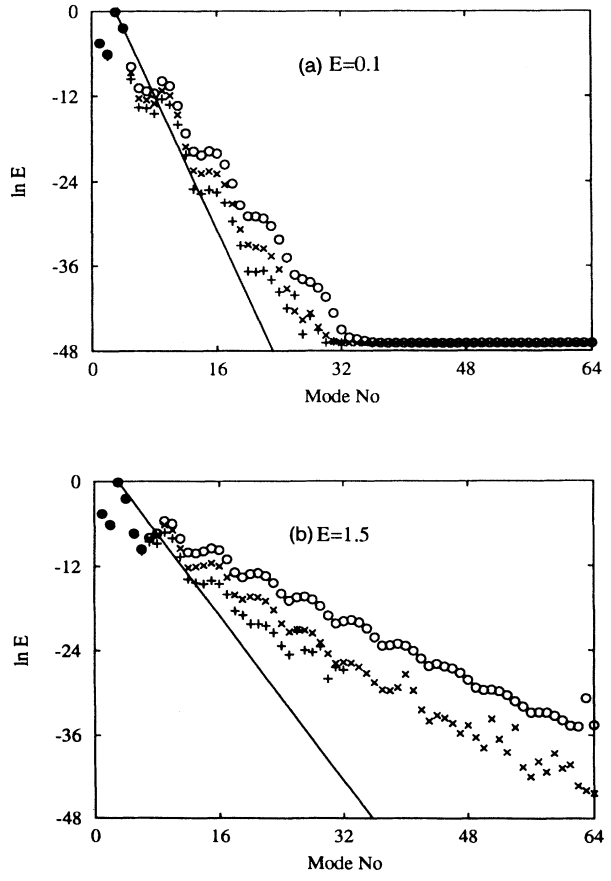

FIG. 1. Natural logarithm of mode energy versus mode number for $N=32$ (pluses), 64 (crosses), and 128 (circles): (a) $E=0.1$ and (b) $E=1.5$.

B. Above the low-energy transition

In Fig. 2 we show the energy in all of the linear modes, for two initial conditions, with $E=3$ and $N=64$. Since $R=12$, low-frequency modes that are coupled can interact strongly. For the circles all of the energy is initially in mode $\gamma=3$. At time $T=N^2/E$ the mode energies have essentially saturated. The general structure of the coupling in which mode h is strongly coupled to mode $h-2\gamma$ as described by (12) is clearly seen. The decrease is geometric as given by (12) and as shown in Fig. 1 at smaller E. There is also a strong coupling between modes 63 and 61, as described by DLL, such that a reverse geometric decreasing regression also takes place, which has imprtant consequences at higher energy as described in Sec. III C below. The couplings do not allow energy to couple to other modes which display zero energy to machine precision. For the pluses, 10% of the energy is placed in modes 2 and 4. This breaks the symmetry, leading to a strong local interaction among the low-frequency modes and consequent multiple geometric couplings that fill in the spectrum. Furthermore, high-frequency peaks appear above the continuum spectrum. As found by DLL, these peaks will continue to grow in time, due to the Arnold diffusion mechanism [20,16,12], but on a time scale that is much longer than that of this figure.

In Fig. 3 we explore the dependence of n_{eff} on $R=6\beta(N+1)E_\gamma/\pi^2$ for values above $R\sim 1$, but for $E=E_c\approx 3$ ($\beta=0.1$). For large N there is a large range of R for which these inequalities hold. The proportionality was already investigated by DLL, but over a narrower range of N. For long times we find $n_{\mathrm{eff}} \geq aR+b$ with $a\simeq 0.5$ and $b=1$, in agreement with previous results. In Fig. 4 a single mode spectrum for $N=128$ and $R=20$ ($E<E_c$) is shown to illustrate the distribution of mode energies that go into a particular n_{eff} (in this case

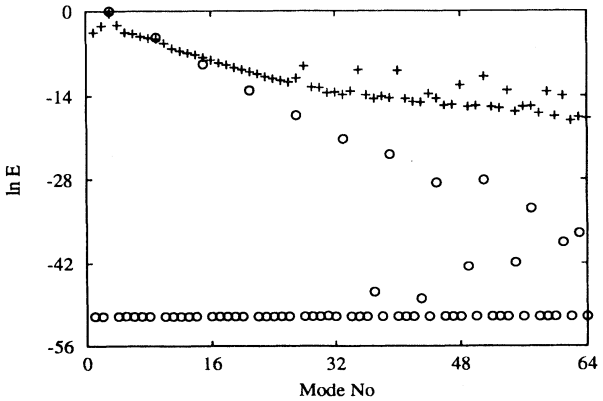

FIG. 2. Natural logarithm of mode energy for $E=3.0$ and $N=64$ and initial energy in mode 3 (circles) and 90% in mode 3 (pluses).

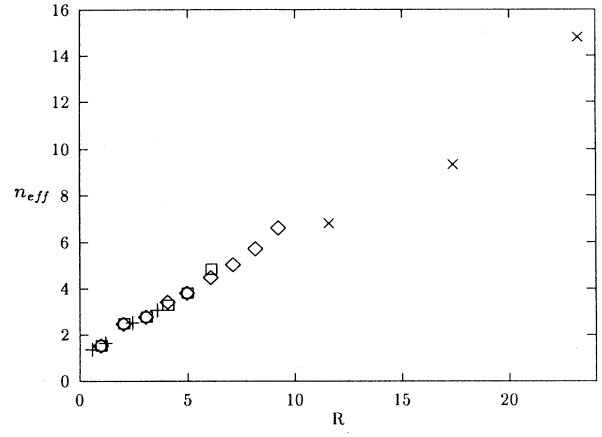

FIG. 3. $n_{\rm eff}$ versus R for four values of N: $N=128$ (crosses), $N=64$ (diamonds), $N=32$ (circles), and $N=16$ (pluses).

$n_{\rm eff}/N=0.072$). The time is sufficiently long that an equilibrium energy distribution has been reached. We shall compare an asymptotic distribution of this type with one at higher energy, for which Arnold diffusion allows equipartition on a longer time scale, but at a time for which a similar value of $n_{\rm eff}/N$ is obtained.

C. Intermediate-energy range

Near the low- to intermediate-energy transition ($E<E_c$ to $E>E_c$) the Arnold diffusion rate is exponentially slow and long observation times are required to observe equipartition. This was done by both KLR and DLL. Here we numerically investigate the scaling well above the energy transition, but within the energy range for which the stochastic diffusion is driven by the fundamental resonance of the mode or few modes that contain most of the initial energy. The time is thus expected to scale with $\tau_b \propto \Omega_b^{-1}$ as in (16). However, kicks on this time scale are driving Arnold diffusion through the coupled chain of N oscillators. We might expect an additional diffusion factor (phase-space filling factor) in the time scale, which is dependnet on the size of the system. We have explored this scaling over a wide range of values of E and N, but holding $E/N<1$ such that strong mode interaction is not involved. In Fig. 5 we plot $n_{\rm eff}(t)$ vs normalized time $\tau \propto t/\tau_b N^{1/2}$ over a range of $10<E<1000$ and $16<N<1024$. The data are essentially within the expected statistical error, indicating that a factor $N^{1/2}$ is a reasonable approximation to the size-dependent filling-factor time scale.

The following argument is used to understand this factor. Suppose the energy is all in the initial mode γ. From (5) it is easy to calculate the Hamiltonian

$$H=\omega_\gamma I_\gamma+\frac{\beta}{2N+2}(\omega_\gamma I_\gamma)^2 \ . \tag{17}$$

The nonlinear term of (17) corrects the linear frequency ω_γ, obtaining $\omega_\gamma+\Omega_b$. If we evaluate the Hamiltonian taking into account that the energy is distributed among the N oscillators we get a time-dependent function containing N independent terms related to the independent angles of the oscillators. Every nonlinear term gives an oscillatory correction to the linear frequency ω_γ, with amplitude of order $(1/N)\Omega_b$. The root-mean-square value of a sum of N such terms is

$$\frac{\partial H_{\rm NL}}{\partial I_\gamma}=\frac{1}{N}\Omega_b\sqrt{N} \ , \tag{18}$$

where $H_{\rm NL}$ stands for the nonlinear term of the Hamiltonian. This result gives the $\sqrt{N}/\Omega_B$ time scaling in agreement with our numerical calculations.

The microscopic details of how $n_{\rm eff}(t)$ is established must still be investigated. In Fig. 6 we give the time-dependent mode spectrum, similar to Fig. 9 of DLL, but for a larger chain ($N=127$) and higher energy ($E=32$). The process of energy transfer into a set of high-frequency modes, followed by transfer to neighboring high-frequency modes, is qualitatively evident. This is in contrast to the result of Fig. 4 for $E<E_c$ in which the energy generally decreases with mode number. The question remains of how the energy locally distributes itself in the two regimes ($E<E_c$ and $E>E_c$) at a given value of

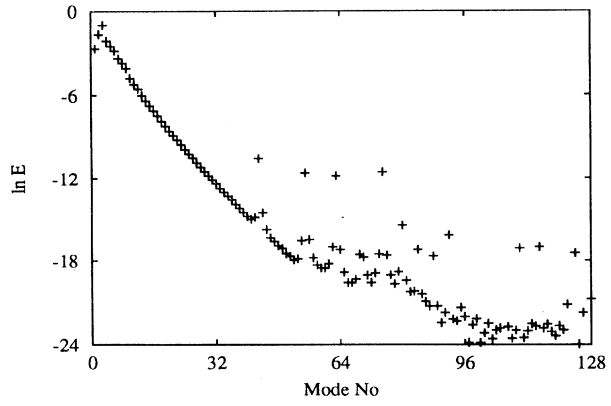

FIG. 4. Natural logarithm of energy vesus mode number for $N=128$ after $t=300N^2/E$ ($E=1.5$).

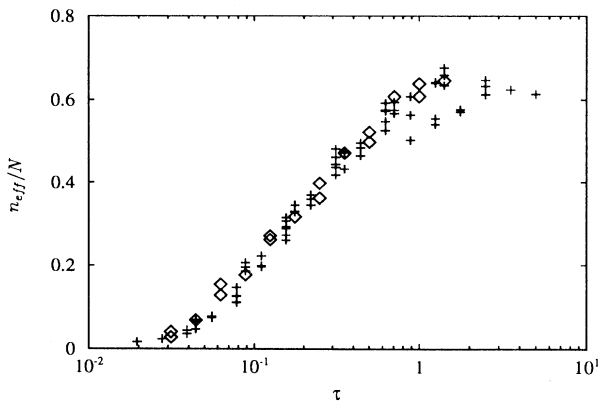

FIG. 5. $n_{\rm eff}/N$ for initial conditions with $16<N<1024$ and $10<E<1000$ versus $\tau=Et/N^{2.5}$.

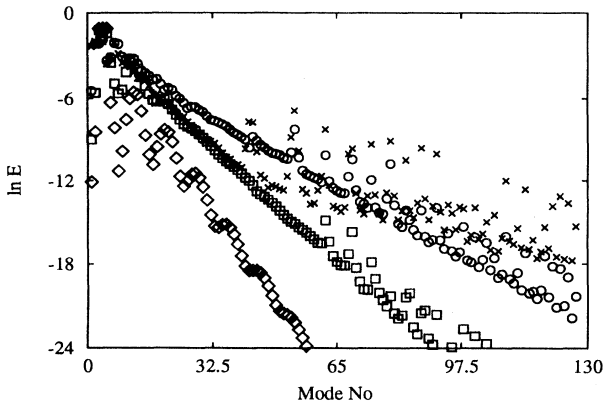

FIG. 6. Four consecutive snapshots of the mode spectrum for $E=32$ and $N=127$.

n_{eff}. We explore this in Fig. 7 by comparing the mode energy distribution at $n_{\text{eff}}/N \simeq 0.1$ obtained for $E_c=3$ with an early-time snapshot for $E=32$ with the same $n_{\text{eff}} \simeq 0.1$. The mode spectra in Fig. 7 show that the high-frequency modes have acquired energy by diffusion, in the $E=32$ case, but are not yet contributing significantly to n_{eff}.

To compare the energy spreading in the few modes around the initial mode with the spreading among the high-frequency modes, we divide the data into two groups, the low-frequency group $1 \le k \le 3\gamma - 1$ and the complementary group $k \ge 3\gamma$. The local values of n'_{eff}/N' for each group are shown in Fig. 8, together with the total n_{eff}/N. As expected, each group separately has larger n'_{eff}/N' than the n_{eff}/N of the total. The few initial modes that contain most of the energy continue to do so through most of the equipartitioning process. The rapid stochastic interchange of energy among a few strongly interacting modes makes the $(n'_{\text{eff}}/N')_g$ of the primary group initially large. The diffusive energy transfer from the low-frequency group to a large rather uniform energy high-frequency group causes the complementary group value of $(n'_{\text{eff}}/N')_c$ to increase in time, although it lies below that of the primary group.

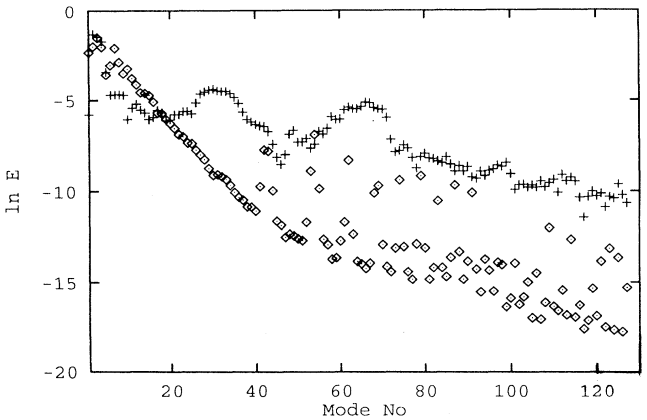

FIG. 7. Mode spectrum at the same $n_{\text{eff}}/N=0.1$ and $N=127$ for $E=32$ (pluses) and $E=3$ (diamonds), at a longer time.

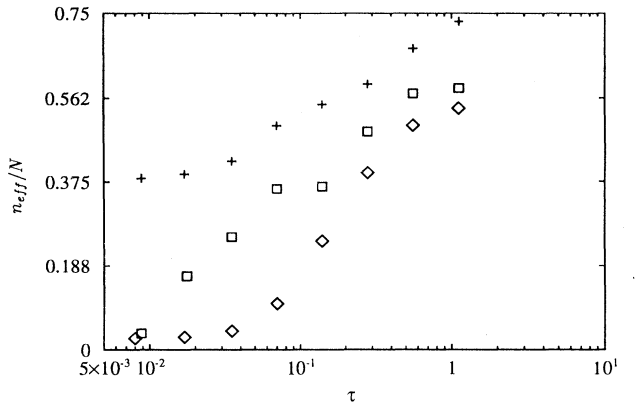

FIG. 8. n_{eff}/N versus $\tau = Et/N^{2.5}$ for three subsets of modes: all the modes (diamonds), low-frequency subgroup (pluses), and complement (squares) for $E=32$ and $N=127$.

IV. CONCLUSIONS AND DISCUSSION

We summarize our understanding of the FPU oscillator chain with strong-spring quartic coupling, in Table I. Unless otherwise mentioned, the initial energy is in a low-frequency mode γ or in a few consecutive modes around mode γ.

The results present a rather complete picture of energy distribution among modes, as observed in computations. Although the numerics have only been presented for energy in mode $\gamma=3$ or for energy in a few low-frequency modes around $\gamma=3$, the results have also been found to hold for other γ's, provided $\gamma/N \ll 1$. The results are also consistent with initial conditions in other studies (see particularly [11]) for which a mode group of initial excitations was used with $\gamma \propto N$ and $\Delta\gamma \propto N$, but still satisfying $\gamma/N, \Delta\gamma/N \ll 1$.

There remain a number of open questions concerning both more complete explanations for numerical results and comparisons with other initial conditions or couplings. One aspect of the numerically observed energy distribution among modes that has not been fully explained within the existing theoretical picture is a rather rapid spreading of energy among neighboring high-frequency modes. The source of this rapid spreading was seen in the comparison of the two initial conditions in Fig. 2 to be related to the spreading of energy among the low-frequency modes. Further study of these couplings with the system closer to equipartition is necessary to understand the scaling with system size. The critical energy for equipartition has been found to be independent of γ, consistent with ergodicity over the energy shell. It would also be interesting to study the case in which energy is initially in a high-frequency mode. In this case the nonlinear high-frequency beat is proportional to Rk^2 and this would couple to the low frequencies $\Omega \sim k$ at $R/(N+1) \sim$ const, which also gives a critical energy independent of N. However, the time scale to reach a particular fraction $n_{\text{eff}}/N =$ const may be different from the case in which the energy is initially in a low-frequency mode. Differences in equipartition time scale, for low-

TABLE I. Phenomena as a function of energy.

Phenomena	Energy range	Characteristic frequency or time scale
Establishing nonlinear modes with a geometric decay among strongly coupled modes $\frac{E_{(1+2n)\gamma}}{E_\gamma} \simeq \left[\frac{3\beta E_\gamma}{4\pi\gamma}\right]^{2n}$	$N\beta E \lesssim 1$	$\tau \sim N/\gamma$ (low frequencies) $\tau \sim N^2/\gamma(\gamma+1)$ (high frequencies)
Formation of local resonance separatrix	$R \equiv (N+1)\frac{6\beta}{\pi}E_\gamma \gtrsim 1$ $(N\beta E_\gamma \gtrsim 1.6)$	$\Omega_b \simeq 6\gamma R/N^3$
Strong stochasticity at resonance separatrix $n_{\text{eff}}/N \simeq \beta E_\gamma$	$R \gtrsim 4$ $(N\beta E_\gamma \gtrsim 6)$	
Arnold diffusion to high-frequency modes on a time scale that is not exponentially slow	Theoretically $\beta E_\gamma > \beta E_c \simeq 1$ Numerically, $E_c \simeq 3$ $(\beta = 0.1)$	At transition, $\Omega_b \sim \Delta\Omega_{12} \simeq \pi^2\gamma/N^2$ Above transition, $\Omega_b \simeq 4\gamma\beta E_\gamma/N^2$
Above transition diffusion to equipartition in time τ_{eq}	$E_\gamma \gg E_c$	$\tau_{\text{eq}} \simeq N^{1/2}/\Omega_B \propto N^{5/2}/\gamma E_\gamma$
Mode overlap leading to rapid equipartition	$\beta E_\gamma > 4N/3\gamma$	$\omega_\gamma = \pi\gamma/2N$

frequency and high-frequency initial conditions, have been observed in the related problem of a chain of coupled pendula [18].

We have investigated the FPU β system, which has a quartic nonlinearity with a positive sign in the Hamiltonian (cubic strong-spring force nonlinearity), to compare most closely to the majority of the numerical work. Recent work with a cubic nonlinearity in the Hamiltonian also indicates the importance of the interaction of the low-frequency resonances [21]. If the sign of β is changed (weak spring), unbounded behavior is also possible. It would be interesting to study this problem in the energy range in which the solutions remain bounded.

ACKNOWLEDGMENTS

The authors would like to acknowledge the support of the Office of Naval Research Grant No. N00014-89-J-1097, the Istituto Nazionale di Fisica Nucleare, the Forum di Fisica Teorica della Materia of the INFM, and an INCOR Grant from the Center for Nonlinear Studies at Los Alamos National Laboratory. Two of us (A.J.L. and S.R.) acknowledge the hospitality of the Institute for Scientific Interchange, Torino, where the collaboration was begun. Our colleagues, H. Kantz, M. Lieberman, and R. Livi have contributed to our understanding of the problem.

[1] E. Fermi, J. Pasta, and S. Ulam, in *Collected Papers of E. Fermi,* edited by E. Segre (University of Chicago, Chicago, 1965).
[2] J. Tuck and M. Menzel, Ad. Math. **9**, 399 (1972).
[3] J. Ford, J. Math. Phys. **2**, 387 (1961).
[4] E. Atlee Jackson, J. Math. Phys. **4**, 686 (1963).
[5] David S. Sholl, Bachelors thesis, The Australian National University, 1991.
[6] F.M. Izrailev and B. V. Chirikov, Dokl. Akad. Nauk SSSR **166**, 57 (1966) [Sov. Phys. Dokl. **11**, 30 (1966)].
[7] R. Livi, M. Pettini, S. Ruffo, M. Sparpaglione, and A. Vulpiani, Phys. Rev. A **28**, 3544 (1983).
[8] R. Livi, M. Pettini, S. Ruffo, M. Sparpaglione, and A. Vulpiani, Phys. Rev. A **31**, 1039 (1985).
[9] R. Livi, M. Pettini, Stefano Ruffo, and A. Vulpiani, J. Stat. Phys. **48**, 539 (1987).
[10] M. Pettini and M. Landolfi, Phys. Rev. A **41**, 768 (1990).
[11] H. Kantz, R. Livi, and S. Ruffo, J. Stat. Phys. **76**, 627 (1994).
[12] J. DeLuca, A. Lichtenberg, and M. Lieberman, Chaos **5** (1) (1995).
[13] C. F. Driscoll and T. M. O'Neil, Phys. Rev. Lett. **37**, 69 (1976), Rocky Mount. J. Math. **8**, 211 (1978).
[14] M. G. Forest, C. G. Goedde, and A. Sinha, Phys. Rev. Lett. **68**, 2722 (1992).
[15] P. Poggi, dissertation, Università di Firenze, 1994; P. Pog-

gi, S. Ruffo, and H. Kantz (unpublished).
[16] A. J. Lichtenberg and M. A. Lieberman, *Regular and Chaotic Dynamics,* 2nd ed. (Springer-Verlag, New York, 1992).
[17] G. Casati, I. Guarneri, F. M. Izrailev, and R. Scharf, Phys. Rev. Lett. **64**, 5 (1990).
[18] C. G. Goedde, A. J. Lichtenberg, and M. A. Lieberman, Physica D **59**, 200 (1992).
[19] M. Falcioni, U. M. B. Marconi, and A. Vulpiani, Phys. Rev. A **44**, 2263 (1991).
[20] Boris V. Chirikov, Phys. Rep. **52**, 265 (1979).
[21] D. L. Shepelyansky (private communication).